

# **Hollow urchin-like metal-organic framework with Ni-O-cluster SBUs as a promising electrode for alkaline battery-supercapacitor device**

Tianqi Chen,<sup>a</sup> Sujuan Bian,<sup>a</sup> Xutian Yang,<sup>a</sup> Wenjie Lu,<sup>a</sup> Kuaibing Wang,<sup>a,\*</sup> Yuxuan Guo,<sup>a</sup> Cheng Zhang,<sup>b</sup> Qichun Zhang<sup>c,d,\*</sup>

## **1. Experimental Section**

### **1.1 Preparation of NiPSC**

Commercially available chemicals were purchased from Acros or TCI and used as received. Solvents were purchased from SCR (Sinopharm Chemical Reagent) and used as received without further purification; water that was used throughout all experiments was purified with the Millipore system (18.2 MΩ cm). The synthesis of NiPSC was prepared according to the reported procedure of PCN-5 single-crystals with slight modification<sup>1</sup>. In a typical synthesis, 0.08 g of H<sub>3</sub>TATB, and 0.2 g of Ni(NO<sub>3</sub>)<sub>2</sub> were dissolved in 6 mL of DMF solution, and the obtained solution was transferred to a Teflon-lined stainless steel autoclave. Then, the autoclave was sealed and placed in a vacuum oven for 48 h at 160 °C. After cooling to room temperature naturally, the resulting product was washed with anhydrous ethanol, ethanol solution (anhydrous ethanol: deionized water=1:1), deionized water, and centrifuged at 10,000 r. After the supernatant was poured off, a green solid was obtained and freeze-dried (Labconco FreeZone) for 12 h. The obtained green nanopowder was named NiPSC.

### **1.2 Preparation of calcined samples of NiPSC**

NiPSC powder (200 mg) was put in a muffle furnace, heated to 500 °C under an air atmosphere with a heating rate of 5 °C min<sup>-1</sup>, and kept at 500 °C for two hours before cooling to room temperature. The product was obtained as a black powder.

### **1.3 Electrode fabrication**

The active material, acetylene black, and polytetrafluoroethylene (PVDF) were mixed (the mass ratio is 75:15:10) together and ground for 30 mins. Then, NMP was added with stirring for 12h to prepare the active slurry. The obtained slurry was uniformly pressed onto the nickel foam (applying area of 1 \* 1 cm<sup>2</sup>) and dried at 80 °C for 2 h under a vacuum oven. After drying, the nickel foam was pressed using a Manual Rolling Press (MR-100A, MTI Corp) to generate the working electrode. The loading mass of the electrode ranged in 2.8~5.4 mg.

### **1.4 Three-electrode test**

The 6 mol L<sup>-1</sup> KOH was employed as the electrolyte, the platinum wire electrode was used as the counter electrode, the Hg/HgO electrode was used as the reference electrode, and the prepared nickel foam electrode was used as the working electrode. The electrochemical performance and cycle performance of the material were tested by cyclic voltammetry (CV), galvanostatic charge-discharge (CP) and electrochemical impedance (EIS) on the electrochemical workstation CHI760e.

### **1.5 Two-electrode test**

A supercapacitor-battery hybrid energy-storage device was assembled using 6 mol L<sup>-1</sup> KOH as the electrolyte, the as-obtained NiPSC as the positive electrode and commercially-available activated carbon as the negative electrode. The electrochemical

performance of the hybrid device was tested using cyclic voltammetry (CV), galvanostatic charge-discharge (CP) and electrochemical impedance spectroscopy (EIS) on an electrochemical workstation CHI760e.

### **1.6 Button battery assembly**

The carbon cloth was heated and refluxed with nitric acid at 80 °C for two hours, then the carbon cloth was placed in deionized water and anhydrous ethanol for ultrasonic 15 min, and the obtained carbon cloth was dried in a vacuum drying oven at 45 °C. The dried carbon cloth was cut into several small discs with a diameter of 14 mm. The active material's slurry and the activated carbon's slurry were uniformly applied to the discs, and dried at 80 °C for 12 h in a vacuum oven. The electrode sheet coated with active material and the electrode sheet coated with activated carbon was obtained. The assembly of the battery is in the following order: positive electrode shell, electrode sheet coated with active material, two filter paper diaphragms with a diameter of 19 mm, electrode sheet coated with a negative electrode material, stainless steel gasket, shrapnel, and negative electrode shell. The positive and negative sides of the diaphragm were added several drops of electrolyte (6 mol L<sup>-1</sup> KOH), and the whole device was sealed using the button battery sealing machine.

### **1.7 Methods and measurements**

The chemical compositions of as-prepared samples were characterized using SEM (S-4800, Hitachi), TEM/HRTEM (JEM-1011, JEOL), XPS (ESCALab MKII X-ray photoelectron spectrometer), EDX (JEM-1011, JEOL), XRD (Bruker D8 Advance), EA (Elementar EL Cube Elemental Analyzer), and FT-IR (Bruker Vector 22). The

adsorption isotherm of nitrogen was measured at 77 K using Micromeritics ASAP 2020 M+C volumetric adsorption equipment. The electrode slurry was loaded on nickel foam and further pressed by Manual Rolling Press (MR-100A, MTI Corp).

The electrochemical measurements were carried out by an electrochemical analyzer system, CHI760E (Chenhua Instrument, Shanghai, China) in a three-compartment cell with a platinum plate counter electrode, a Hg/HgO reference electrode and a working electrode. The electrolyte was a 6.0 M KOH aqueous solution and electrochemical impedance spectroscopy (EIS) measurements of as-synthesized samples were conducted at an open-circuit voltage in the frequency range of 100 kHz ~ 10 mHz.

### **1.8. Working mechanism of battery-type NC/NiCo electrode**

Based on the modified power-law equation (1) referred from the Dunn group, the possible working mechanism for NiPSC electrode was listed below:

$$\log i = b \log v + \log a \quad (1)$$

where  $i$  and  $v$  represent the current and sweep rate separately. The simulated  $b$  values range between the value of 0.5 (diffusion-controlled process) and 1.0 (surface-controlled process), indicating that the battery-type behavior of NiPSC electrode combines two separate mechanisms simultaneously.

Following the previous approach reported by the Dunn group, the above two mechanisms in the equation can be combined as follows:

$$i(V)/v^{1/2} = k_1 v^{1/2} + k_2 \quad (2)$$

These two separate mechanisms can be determined quantitatively.

## 2. Structural Characterizations

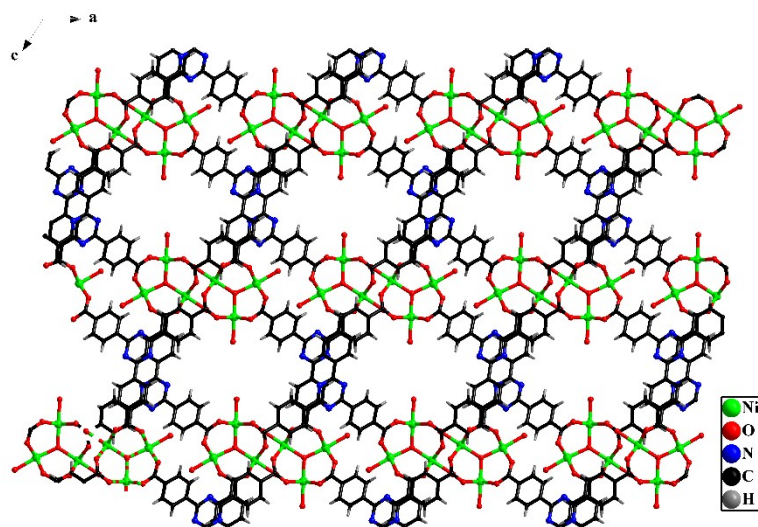


**Fig. S1** Crystal structure of NiPSC material viewing along with the (020) facet by using reported CIF format.

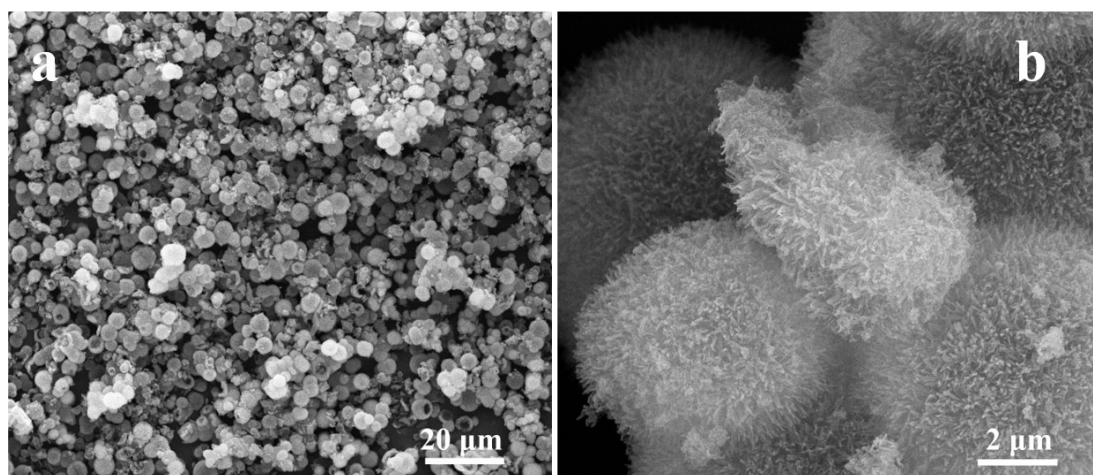


**Fig. S2** (a-b) SEM images of NiPSC material.

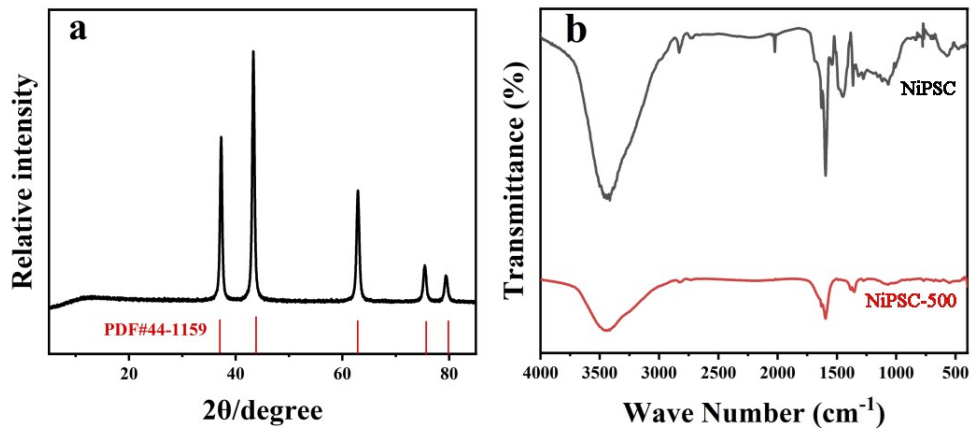


**Fig. S3** (a) Comparison of the Infrared spectra of NiPSC and its calcined sample. (b) Comparison of the Infrared spectra of NiPSC and its calcined samples (marked as NiPSC-500).

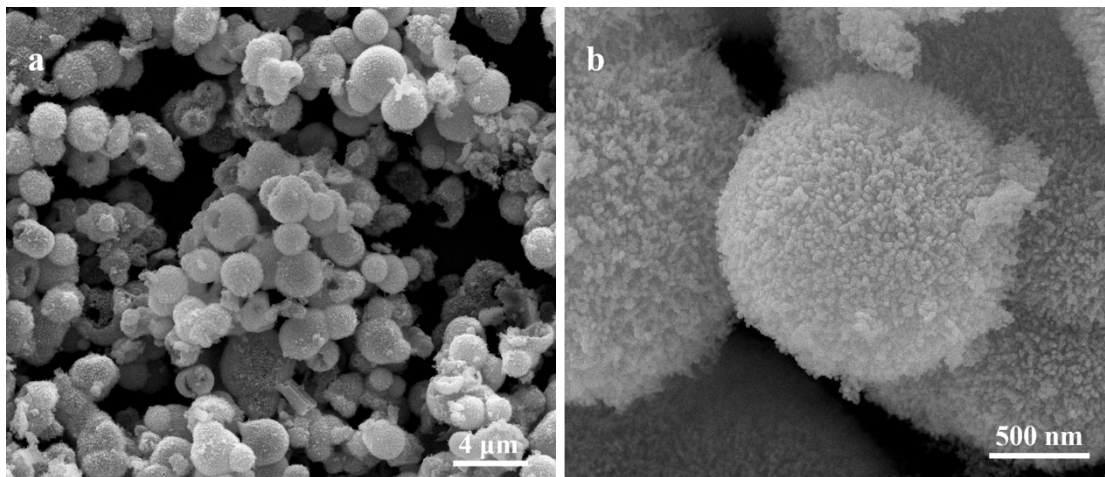


**Fig. S4** (a) SEM image of NiO material. (b) Enlarged SEM image of NiO.

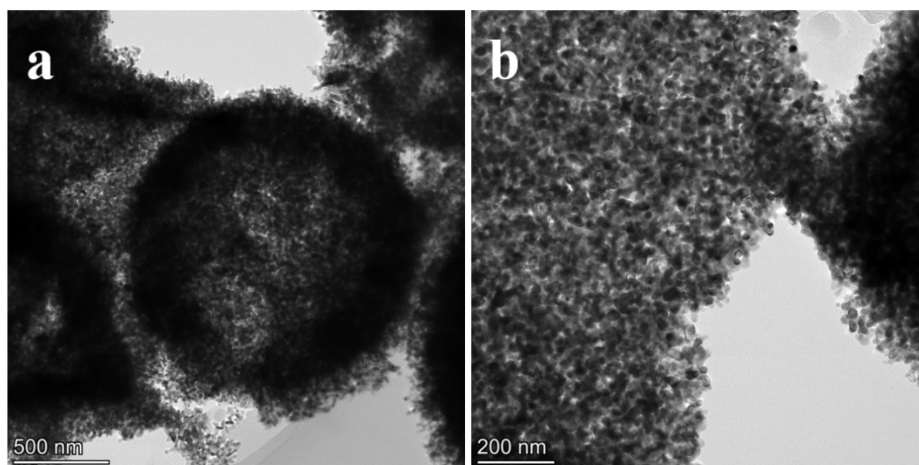


**Fig. S5** (a-b) TEM images of NiO material.

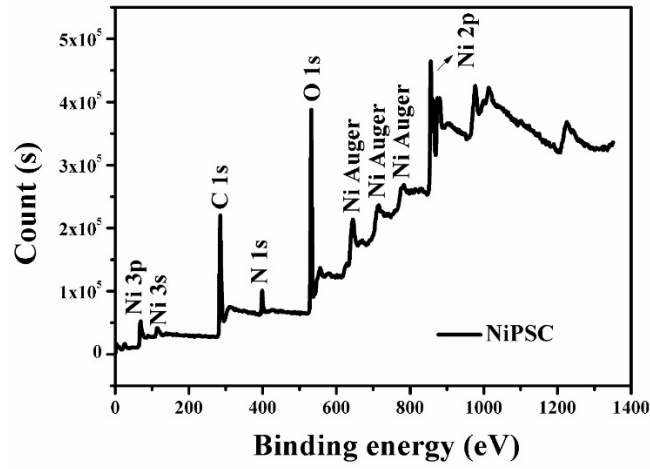


Fig. S6 XPS survey spectrum of the as-obtained NiPSC.

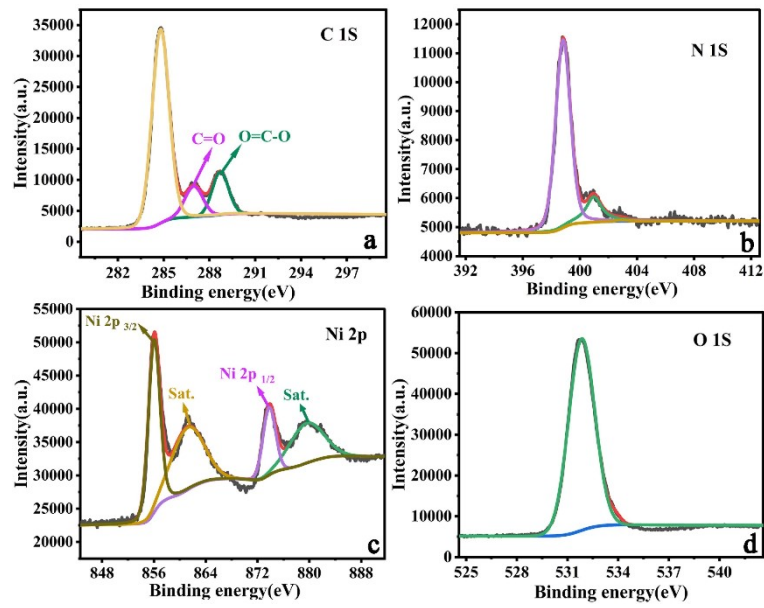
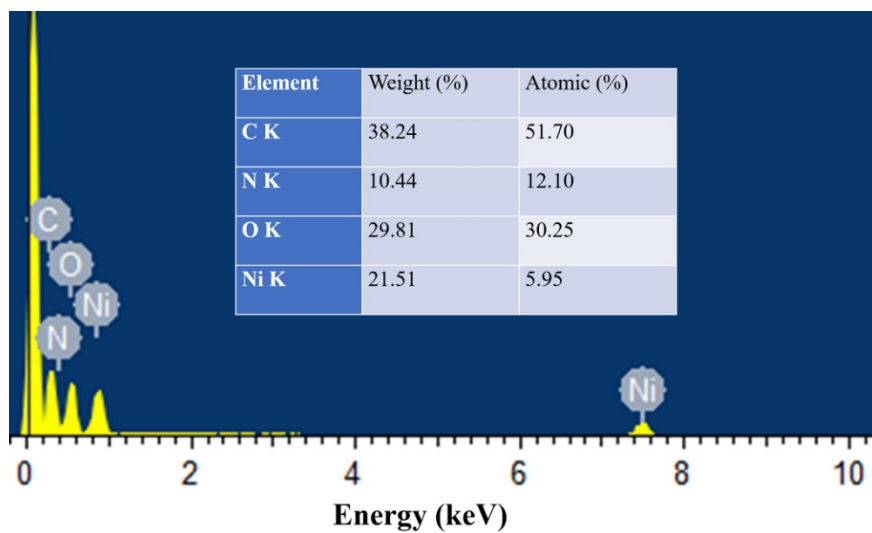
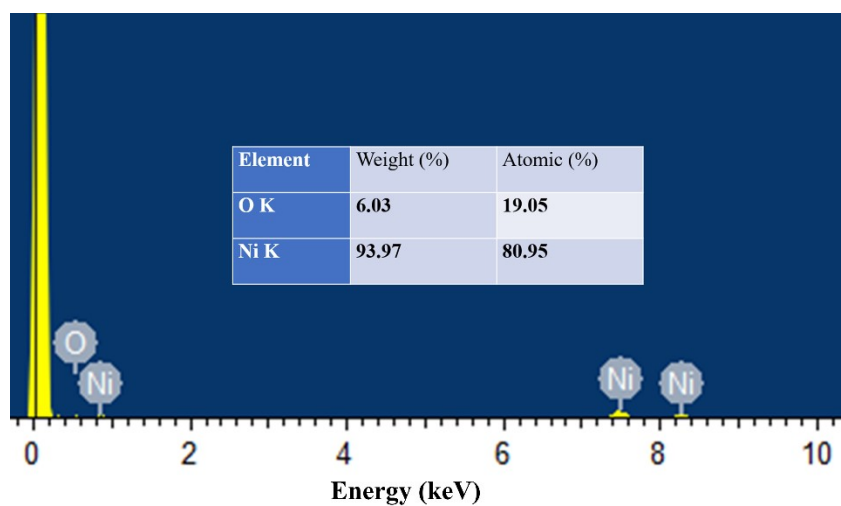


Fig. S7 High-resolution XPS spectra of (a) C 1s, (b) N 1s, (c) Ni 2p and (d) O 1s.



**Fig. S8** High-resolution XPS spectra of (a) C 1s, (b) N 1s, (c) Ni 2p and (d) O 1s.



**Fig. S9** High-resolution XPS spectra of (a) C 1s, (b) N 1s, (c) Ni 2p and (d) O 1s.



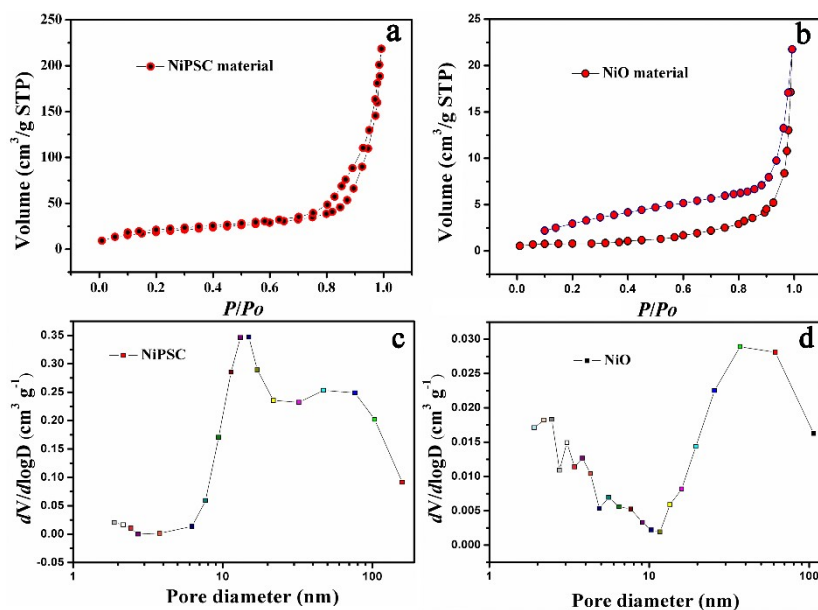


**Fig. S10** (a,b) The nitrogen adsorption-desorption isotherm. (c,d) The pore size distributions.

**Table S1** Comparison of specific surface area and pore-size of materials

	Ni-PSC	NiO
BET ( $\text{m}^2 \text{g}^{-1}$ )	66.70	2.391
Average pore diameter (nm)	22.46	10.85
pore volume ( $\text{cm}^3/\text{g}, V_{\text{total}} - V_{\text{mic}}$ )	0.340	0.033

### 3. Electrochemical performances and working mechanism

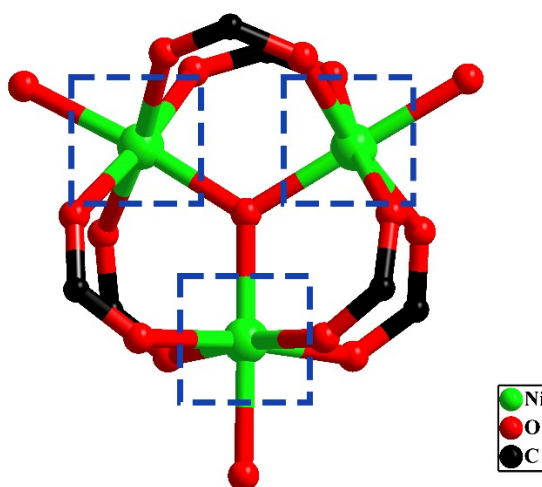


**Fig. S11** The  $\text{Ni}_3(\mu_4\text{-O})$  cluster formed by three Ni atoms bridging one oxygen atom.

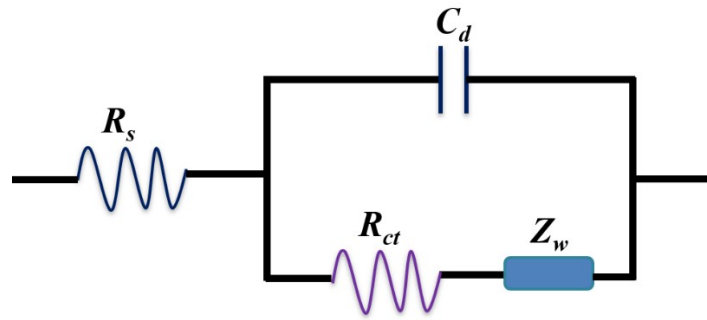


Fig. S12 The equivalent circuit for simulating the EIS data.

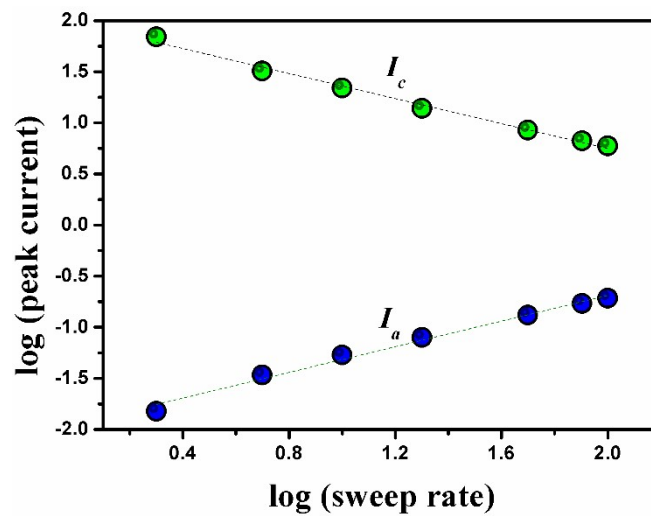


Fig. S13 Power law dependence of current on sweep rate for NiPSC electrode.

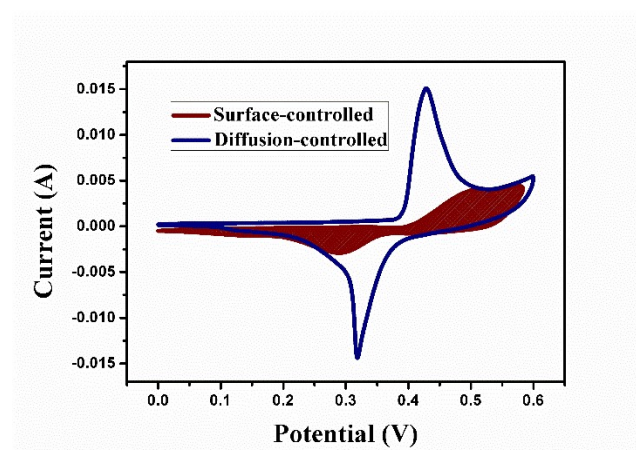
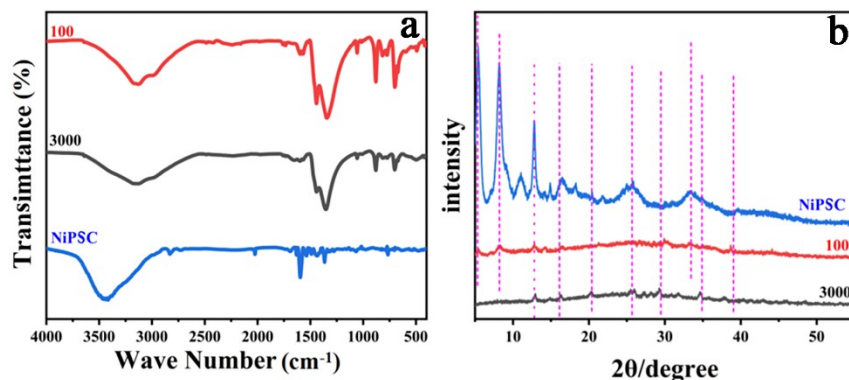
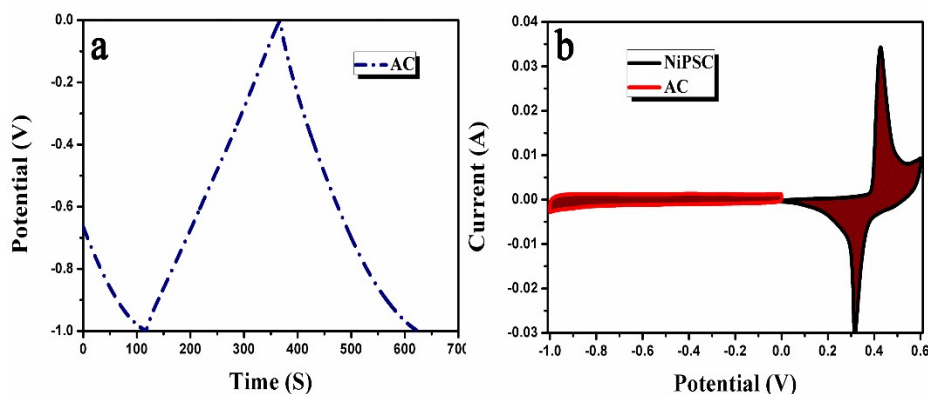


Fig. S14 Voltammetric response for the as-prepared NiPSC electrodes at a sweep rate of  $2 \text{ mV s}^{-1}$ .



**Fig. S15** (a) Comparison of the Infrared spectra of NiPSC and samples with 100 cycles and 3000 cycles. (b) Comparison of XRD patterns of NiPSC and samples with 100 cycles and 3000 cycles.



**Fig. S16** (a) CP curves of AC at a current density of  $0.5 \text{ A g}^{-1}$  in  $6 \text{ mol/L KOH}$ . (b) CV curves of AC and NiPSC at a scan rate of  $5 \text{ mV s}^{-1}$

**Table S2** Compared data on power and energy density with reported references.

Device	Power Density ( $\text{W kg}^{-1}$ )	Energy Density ( $\text{Wh kg}^{-1}$ )	Ref.
Ni-Co SNWs//AC	447	25	41
NiCo-MOF@PNTs//AC	375	41.2	42
NiCoS/NF-1//AC	376	11.6	43
CNF@Ni-CAT//AC	297	18.67	44
NiHPi-500//AC	7242	18	45
NiCo-MOF//AC	800	20.9	46
<b>NiPSC//AC</b>	<b>425</b>	<b>28.18</b>	This work

## References

1. S. Ma, X. S. Wang, E. S. Manis, C. D. Collier and H. C. Zhou, Metal-organic framework based on a trinickel secondary building unit exhibiting gas-sorption hysteresis, *Inorg Chem*, 2007, **46**, 3432-3434.

